Isochiral Form II of Syndiotactic Polypropylene Produced by Epitaxial Crystallization

J. Zhang and D. Yang

State Key Laboratory of Polymer Physics and Chemistry, Changchun Institute of Applied Chemistry, Chinese Academy of Sciences,159, Renmin Street, Changchun 130022, China

A. Thierry, J. C. Wittmann, and B. Lotz*

Institut Charles Sadron (CNRS-ULP), 6, rue Boussingault, F- 67083 Strasbourg, France

Received May 2, 2001; Revised Manuscript Received June 18, 2001

ABSTRACT: Epitaxial crystallization of syndiotactic polypropylene (sPP) on 2-quinoxalinol (2-Quin) yields, in the lower part of the crystallization range, the less common and metastable form II based on the packing of isochiral helices, rather than the stable antichiral form I. The contact plane is $(110)_{II}$. Form II exits only as a thin layer ($< \approx 50$ nm) near the substrate surface. During further growth away from the surface, a transition takes place to the disordered form I, observed in "conventional" thin film growth. The epitaxial relationship rests only partly on dimensional matching with the chain axis repeat distance (which would be valid for both forms I and II) and on interchain distances. Whereas a better dimensional match would be achieved with form I, selection of the isochiral form II results from better correspondence of the surface topographies of the deposit $(110)_{II}$ sPP and substrate 2-Quin (001) contact faces.

1. Introduction

Syndiotactic polypropylene (sPP) exhibits a complex crystalline polymorphism based on different chain conformations and packing schemes.[1] The more stable chain conformation is of the type trans−trans-gauche−gauche (ttgg or t_2g_2). The chains pack in two different, but highly correlated orthorhombic unit cells: a two-chain unit cell made of isochiral helices,[2] and a four chains unit cell (with a doubling of the *b* parameter) with full antichiral packing of helices along both *a* and *b* axes[3] (Figure 1). The former unit cell and isochiral crystal structure (space group $C222_1$) (now known as form II) was initially proposed as the only crystal structure of sPP on the basis of X-ray fiber studies of stretched and annealed sPP,[2] but was found later to be a less stable polymorph.[3,4] The stable antichiral form now known as form I is produced upon crystallization from the bulk, in its purest form with highly syndiotactic polymers only, and crystallized at high crystallization temperatures (e.g., 145 °C).[3,4] At lower T_cs, a packing disorder sets in, whereby the isochiral packing becomes mixed with the antichiral one.[3−7] As a consequence, 2.8 Å (i.e., $b_{II}/2$ or $b_I/4$) shifts of layers along the *b* axis are introduced, which are revealed by a characteristic streaking along the 02*k*0 layer line of the *hk*0 diffraction pattern. The crystal structure of the stable antichiral form I has been improved in successive steps. According to De Rosa et al.,[6] the high symmetry initially considered (*Ibca*)[3] should be reduced to $P2_1/a$. The differences are relatively minor, however, and the simpler model with *Ibca* symmetry can be considered as a prototypical model for the stable structure of sPP.[8]

The isochiral form II is more elusive, and has been observed so far only under specific deformation treatments (e.g., in fibers),[2] or at elevated pressures.[9] It appears to be the result of a crystal−crystal transformation from an extended chain conformation of sPP (the crystalline form III, produced on stretching the fiber) to the ttgg form (produced during the high temperature annealing). The transformation is a solid-state one. It

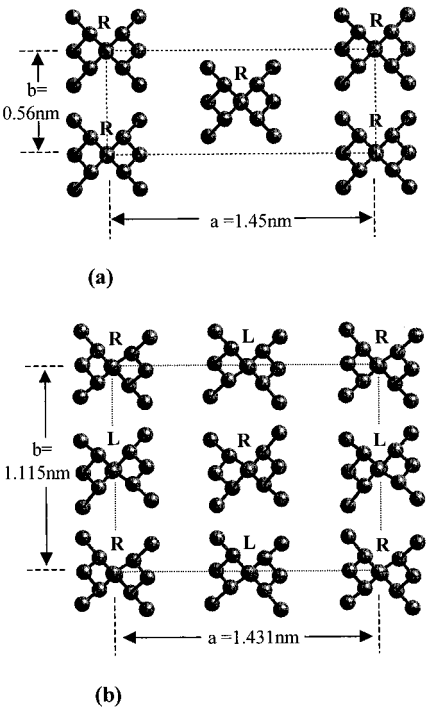

Figure 1. Two crystal structures of syndiotactic polypropylene based on the ttgg chain conformation. (a) C-centered form II made of isochiral helices, according to Corradini et al.[2] Cell parameters: $a = 1.45$ nm, $b = 0.56$ nm, $c = 0.74$ nm, space group $C222_1$. (b) Base-centered form I with full antichiral packing of helices along *a* and *b* axes. The slight distortion of helices is as suggested by De Rosa et al.[6,7] Monoclinic unit cell, cell parameters: $a = 1.431$ nm, $b = 1.115$ nm, $c = 0.75$ nm, $\gamma = 90.3°$, space group $P2_1/a$. Note that throughout this paper, we adopt the terminology suggested by De Rosa et al.[6] to characterize the various crystal modifications of sPP.

* To whom correspondence should be addressed. E-mail: lotz@ics.u-strasbg.fr.

10.1021/ma010758i CCC: $20.00 © 2001 American Chemical Society
Published on Web 08/04/2001

starts from a linear conformation and ends up in a helical conformation: neighbor chains are transformed cooperatively due to topological constraints, which implies that the transformation is a chiral process,[10] thus accounting for the observation of the chiral form II in the fibers only. This preferential formation of the chiral structure has indeed been monitored in recent studies.[11]

This issue of chiral vs antichiral packing is actually a quite general one in the family of syndiotactic polyolefins. As an illustration, the stable forms of sPP and of syndiotactic poly(1-butene) (sPBu-1), which share the same t_2g_2 chain conformation, do differ in this respect: fully antichiral for sPP, and chiral for sPBu-1.[12]

In a different context, *epitaxially induced crystallization of polymers* is a convenient means to generate unstable or metastable crystal modifications of a number of polymers.[14] Indeed, when lattice matching between the substrate and polymer is more favorable, the metastable modification may be generated and can be obtained in high yield (e.g., >98% for isotactic polypropylene, β phase).[13] However, this metastable form may exist only as a thin transient layer near the substrate surface when a growth transition to a more stable form takes place during additional growth, away from the substrate. For example, a conversion from the monoclinic to the orthorhombic form is observed for polyethylene crystallized on NaCl[15] and a variety of organic acids and salts.[16] For polyoxymethylene, the metastable orthorhombic phase gives rise to the stable hexagonal phase.[17]

Epitaxial crystallization of sPP has already been achieved, using *p*-terphenyl as a substrate.[18] The stable, antichiral form I is produced. Atomic force microscopy imaging of its *bc* contact face revealed individual stems with alternating right and left helical hands, thus confirming in real space the antichiral packing in the unit cell.[18] In this paper, we report on the epitaxial crystallization of sPP on another substrate, namely 2-quinoxalinol (2-Quin). This substrate was already used to induce the epitaxial crystallization of isotactic poly(1-butene)[19,20] and isotactic poly(4-methyl-pentene-1).[21] It happens that the *b* axis repeat distance of 2-Quin (7.35 Å) provides a potential match with the chain axis repeat of the ttgg helical conformation of syndiotactic polymers (≈7.4 Å). As shown in this contribution, such ttgg chain conformations of sPP are indeed obtained. However, the less common, isochiral polymorph (form II) of sPP is produced, but mostly as a transient layer near the substrate surface, and in the low T_c range. The preferential development of this metastable chiral form II is analyzed by comparing the contact plane surface topographies of forms I and II of sPP and the matching contact plane of 2-quinoxalinol.

2. Materials and Experimental Procedures

Samples of syndiotactic polypropylene of various origins have been used throughout this study, but results will be reported for a very high syndiotacticity sample (>99% racemic triads) provided by Dr. T. Simonazzi (Himont, Italy) and already used in previous investigations.[4, 18]

2-Quinoxalinol

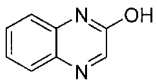

is of commercial origin (Aldrich) and was used without further purification.

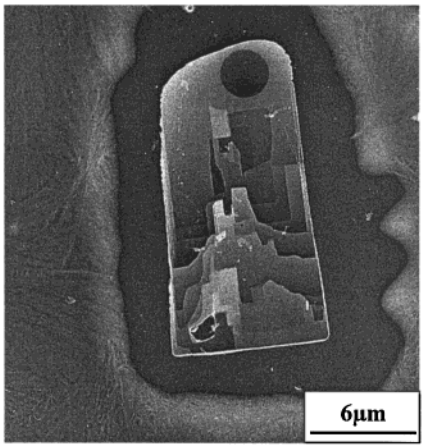

(a)

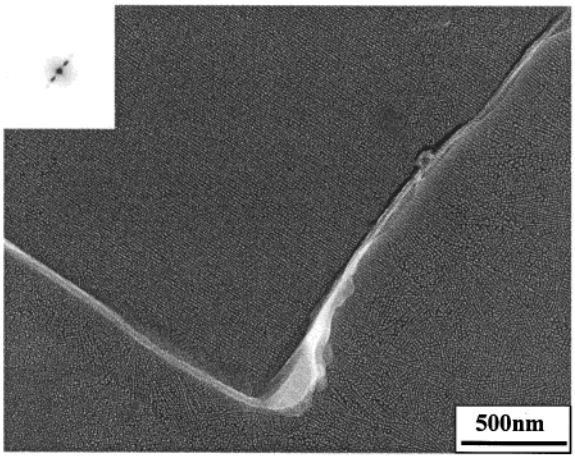

(b)

Figure 2. (a) Electron micrograph of a crystal of 2-quinoxalinol deposited by sublimation/condensation on a thin film of sPP. In the present case, the crystal has "sucked in" the surrounding sPP. The round overexposed area near the top of the crystal is typical of areas selected to record the diffraction patterns shown in Figure 3. (b) Epitaxially crystallized thin film of sPP on the corner of a crystal of 2-quinoxalinol, as observed in transmission electron microscopy after dissolution of the substrate and decoration of the sPP contact face with gold vapors (gold decoration technique). The particles of gold gather in the interlamellar regions and reveal the lamellar periodicity. Insert: low angle electron diffraction pattern of the epitaxially crystallized film (actually of the pattern of decorating gold particles), in proper relative orientation, and indicating a lamellar periodicity of ≈ 16 nm. Note the slight extension of the sPP lamellae beyond the lateral limit of the 2-Quin crystal but the absence of nucleating effect along the bottom edge of the crystal.

The experimental procedures are by now well established.[14] A thin polymer film is spread on a glass cover slide by evaporation from a dilute (≈1%) solution in *p*-xylene. Single crystals of the low molecular weight substrate—in this study, 2-quinoxalinol—can, on account of its high vapor pressure, be deposited by sublimation/condensation on the sPP film (Figure 2a). The polymer−substrate "sandwich" film is melted and recrystallized at predetermined crystallization temperatures. The substrate is dissolved in hot ethanol, leaving a thin polymer film with the imprint of the substrate crystals, and with the contact face exposed. These films are (if desired) either shadowed with Pt−carbon or gold-decorated, backed with a carbon film, removed from the glass cover support with the help of a poly(acrylic acid) backing, floated on water, and mounted on electron microscope grids.

Electron microscopic observations are performed in the defocused electron diffraction mode with a Philips CM12 microscope operated at 120 kV. The very low magnification used (usually ≈×600) helps to limit electron beam damage of the polymer. Electron diffraction is mostly performed on specimens mounted on a rotation-tilt stage (±60°). The crystal structures and diffraction patterns are modeled with the different modules of the Cerius 2 program (Molecular Simulations, Waltham, MA, and Cambridge, U.K.).[22]

3. Results

(a) Crystallization in the Low T_c Range (T_c < ≈ 110 °C). Crystallization procedures described in the Experimental Section yield thin polymer films which display lamellar crystals standing edge-on in the areas in contact with the nucleating agent (Figure 2b). The lamellar thickness can be estimated from Pt/C shadowed samples, but it is equally accessible by small angle diffraction of gold-decorated samples. The vaporized gold gathers indeed in the ditches made by the interlamellar amorphous material and produces a regular striped pattern of rows of gold particles which is suitable for both direct observation (Figure 2b) and for small angle electron diffraction (Figure 2b, inset). The lamellar thickness is in the range of 16 nm.

The *diffraction patterns* obtained from the epitaxial film of sPP are more intriguing (Figure 3). When untilted, the diffraction pattern displays the 002 reflection characteristic of the stable ttgg chain conformation of sPP (Figure 3a). However, the equator is nearly "empty", which indicates that the contact plane is *not* a "simple" plane parallel to either *ac* or *bc*. Further evidence about the film structure must be gathered by resorting to tilting experiments, with the c_{sPP} axis as the tilt axis. The most informative diffraction patterns obtained under these conditions correspond to tilt angles of ≈+20 and −50° around *c* (Figure 3, parts b and c, respectively). These tilt angles are indicated with respect to the form II and I structures in Figure 3d.

Analysis of these data is a priori rather complex, since we are dealing with two crystal forms of sPP (forms I and II) that share the same cell geometry. They differ only by the doubling of one cell parameter (the *b* axis) and, of course, by a different space group symmetry. In the analysis, we use for form II the "standard" unit cell due to Corradini et al. (Figure 1a).[2] For form I, several slightly different chain geometries (distorted or undistorted) and chain packings (and thus space groups) have been considered. As indicated in the Introduction, whereas the highest possible symmetry of the unit cell is *Ibca*,[3] De Rosa et al.[6] have considered a lower symmetry ($P2_1/a$) (Figure 1b). However, in view of their geometrical and dimensional similarities, forms I and II of sPP share a number of common reflections (same spacing, same location in reciprocal space), which are not therefore expected to be discriminative. These reflections are indexed as *hkl* in form II and *h*2*kl* in form I. Fortunately, however, most of the analysis can be based on the sole *hk*0 reflections of the two forms, which are clearly different. The patterns expected for forms II and I are displayed in Figure 4, parts a and b, respectively. They are explored in the present case by tilting the sample in the specimen stage, with c_{sPP} as the tilt axis: the sections of the reciprocal space to be discussed are shown in the *hk*0 patterns of Figure 4a.

Anticipating conclusions to be drawn next, the analysis suggests that the epitaxially crystallized film of sPP is in form II, i.e., in the less familiar chiral form.

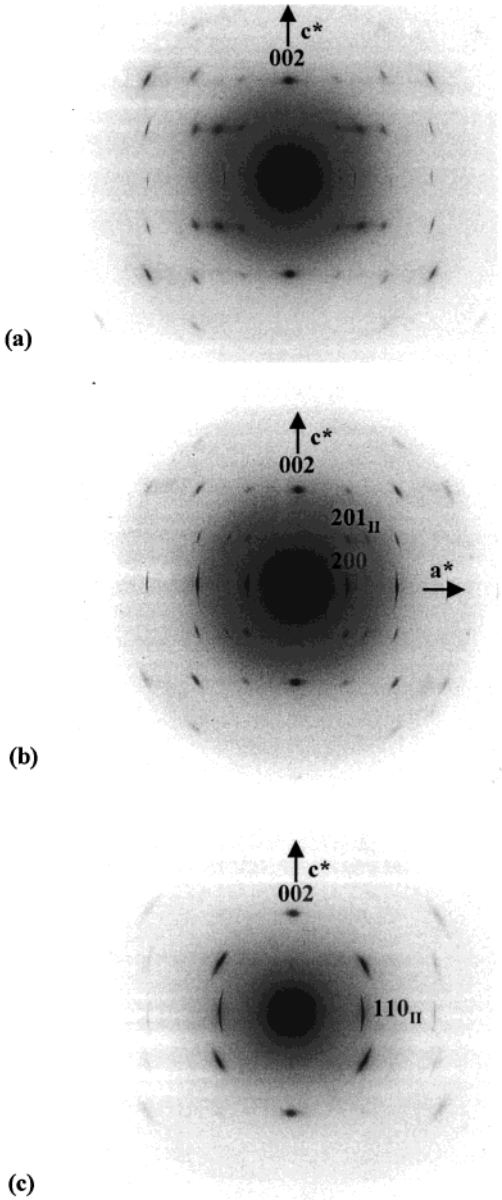

Figure 3. Diffraction patterns of the sPP thin film epitaxially crystallized on 2-Quin crystals, as observed for different tilts relative to the chain axis (vertical). (a) untilted film (b) tilted 20° (clockwise) about *c* (c) tilted 50°, counterclockwise about *c*.

Furthermore, the contact plane is of type {110}, i.e., at some 21° to the *ac* plane of the unit cell (Figure 1a). The epitaxial relationship is summarized as follows.

Contact planes:

$$\{110\}_{sPP,form\ II} \,//\, (001)_{2\text{-quinoxalinol}}$$

Orientations in the plane:

$$[001]_{sPP,form\ II} \,//\, [010]_{2\text{-quinoxalinol}}$$

The structural analysis rests on the following features (concentrating in a first step on the most prominent of them).

•As indicated, the contact plane includes neither the *a* axis nor the *b* axis of either form I or form II unit cells of sPP, since the equator of the untilted sample is "empty". The first layer line is more populated, but its analysis is deferred to a later stage

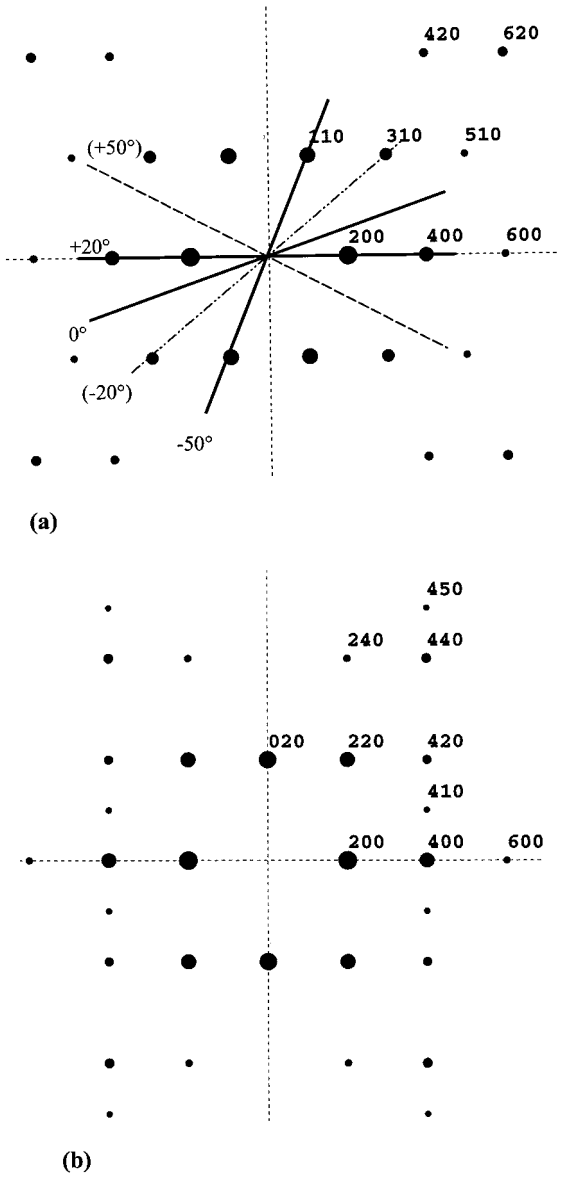

Figure 4. Schematic representation of the *hk*0 diffraction patterns of sPP in form II (a) and I (b). The bold lines correspond to sections of the reciprocal space generated by the tilts indicated. Note that the contact plane is *either* (110) *or* ($\bar{1}$10). This in turn means that for any one tilt (e.g., +20 or +50°), *two* sections of the reciprocal plane are explored. The second sections are similar to the ones shown here as −20° and −50°.

•A tilt of ≈ +20° brings the *ac* plane into a diffracting position; i.e., the *b* axis becomes the zone axis (Figure 3d): the pattern (Figure 3b) is characterized by a strong equatorial reflection, of spacing 7.2 Å, indexed as 200 *for both forms I and II*. Possible discrimination between the two forms comes from the corresponding reflection on the first layer line: 201, spacing 5.16 Å. This reflection is forbidden by the space group symmetry of form I but is expected for form II.

•Presence of form II is further supported by the diffraction pattern obtained at −50° tilt (Figure 3c). The equatorial reflection, at 5.22 Å, is a very discriminative reflection indeed: it must be indexed as 110_{II} (Figure 4a). No such reflection is expected for form I (Figure 4b). Note also that this is the *only discriminative tilt* at which some intensity is recorded on the equator (the 20° tilt, which yields the 200 reflection *common* to forms I and II, is *not* discriminative). In Figure 3c, the corresponding reflection on the first layer line (indexed as 111_{II} and 121_{I}) is, again, *not* discriminative since it is strong for both crystal forms.

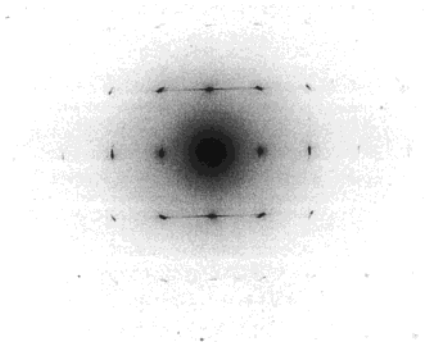

Figure 5. Electron diffraction pattern of crystals grown in the bulk under the same crystallization conditions as the epitaxially crystallized film of sPP. Note the conspicuous presence of diffraction spots indicating a predominantly form I crystal structure (compare with Figure 4b), as well as the characteristic streaking indicating 2.8 Å shifts of layers along the *b* axis.

•If we accept that the contact plane is oriented at some 20° to the *ac* plane of either forms I or II, and if the film is in form I, then equatorial reflections of form I should be observed at tilt angles of 32° (220_{I}, spacing 4.4 Å), and 70° (020_{I}, spacing 5.6 Å). The stronger 020_{I} reflection cannot be accessed since it is outside the range of the tilting stage (±60°). However, no reflection is observed for the 32° tilt, which rules out the presence of any significant fraction of form I in the epitaxially crystallized film.

•One feature must be mentioned, which complicates, but does not amend the above conclusions. In any one epitaxially crystallized film, both structurally equivalent $(110)_{II}$ and $(\bar{1}10)_{II}$ contact planes coexist. Any tilt of the specimen by an angle θ therefore samples not one, but two, sections of the reciprocal space (indicated in Figure 4a as + and − θ). This gives rise to additional rows of *hkl* reflections, in particular 31*l* ones for the 20° tilt. These tilts, however, sample sections of the reciprocal space with much weaker reflections (on account of their lower structure factor). While present in the patterns, these reflections are not commented on any further.

The analysis just developed indicates that the less common form II is produced as a result of epitaxial interactions. However, under the crystallization conditions used, this form II is *not* formed spontaneously. The "natural" crystal form develops in the large areas of the sPP film that are not in contact with 2-Quin crystals. These areas display spherulites and single crystals, which yield *hk*0 diffraction patterns as shown in Figure 5. The patterns display the by now classical sharp $2h00_{I}$ set of reflections and the streaks parallel to *h*20, with significant reinforcements at positions corresponding to 020_{I} and 220_{I}. They indicate a form I crystal structure, with a significant impact of 2.8 Å ($b_{II}/2$ of form II or $b_{I}/4$ of form I) shifts of layers generated by inclusion of "isochiral mistakes" in the antichiral packing of form I.[4,5]

Under the same crystallization conditions, significantly different crystal structures are therefore produced by epitaxial crystallization and in the bulk. This raises the issue of the *perennity* of the epitaxially induced, unstable form as growth proceeds into the bulk material, away from the substrate surface, and influence

of the latter fades away. Such a transition from a "pure" form II as obtained by epitaxy to form I (characteristic of bulk crystallization) appears structurally possible and even likely. Indeed, the disorder of form I mimics the shifts of layers characteristic of form II. At what distance from the substrate surface does this type of transition occur? No precise answer can be given at this stage, but two experimental observations are relevant to this issue.

•No significant presence of form I is detected in epitaxially crystallized films; i.e., form II is preserved up to at least the maximum film thickness acceptable in transmission electron microscopy (≈50 nm).

•Transcrystalline layers (induced by epitaxial growth) that develop on the edges of the 2-Quin crystal make it possible to investigate the transition to "bulk" growth further away from the substrate. In Figure 2b, the transcrystalline strip extends about 200 nm into the melt adjacent to the lateral edge. The epitaxial origin of the transcrystalline strip is indicated by the edge-on lamellar orientation. We believe that these transcrystalline layers give rise to a feature of the pattern in Figure 3a not discussed so far. Most patterns taken at 0° tilt display only reflections characteristic of the epitaxy. In addition to these reflections, Figure 3a displays a relatively sharp 020_I reflection on the equator (and corresponding 0*kl* reflections). The presence of these extra reflections suggests that the area selected encompasses some transcrystalline domains, which is consistent with the fact that the chain axis orientation parallel to the substrate is preserved. At the same time, this additional growth differs in two respects from the epitaxial film: (a) growth takes place in form I and (b) the *b* axis is now oriented parallel to the support surface rather than at a significant angle to it (70°). Both features are expected in bulk crystallization; in particular, reorientation of the *b* axis in the plane of the thin film is fully consistent with the fact that it is by far the fastest growth direction under the present crystallization conditions.

To conclude this section, therefore, epitaxial crystallization of sPP on 2-Quin crystals generates the metastable, chiral form II rather than the antichiral form I formed in the bulk under similar crystallization conditions. A growth transition (progressive or abrupt) from form II to form I must take place away from the substrate surface, when bulk crystallization conditions prevail. Present results, although not fully conclusive, suggest that form II generated by the epitaxy extends further in the bulk than, e.g., the monoclinic form of polyethylene (which is limited to a few nanometers). This robustness appears to be due to the fact that the two phases have very comparable energies. However, our data also confirm the specificity of 2-Quin toward the sole form II of sPP. The origin of this specificity toward form II is analyzed in a later section by comparing the surface topographies of the interacting contact planes. First, however, the changes introduced by varying the crystallization conditions are briefly reported.

(b) Crystallization at Higher T_cs (T_c > 110 °C). The behavior just described is valid for relatively low crystallization temperatures. When increasing T_c to ≈130 °C, epitaxial crystallization of sPP on 2-Quin is no longer observed. This result is not surprising, however, since most nucleating agents become inactive in the high T_c range of the polymer. In the present case, an additional feature may play a role. As the crystallization temperature increases, the "natural" crystal phase of sPP (assessed above with the help of *hk*0 electron diffraction patterns of flat-on lamellae) becomes a progressively "purer" form I, less "spoiled" by the structural disorder associated with the 2.8 Å shift of layers reminiscent of form II packing. In other words, the crystalline modification that would be induced by epitaxy, i.e., form II is, at high T_cs, more remote from the "natural" crystal form I characteristic of those T_cs. Therefore, it is not surprising that the epitaxy described so far for low T_cs is no longer observed at high T_cs.

4. Discussion: Crystal-Form Specific Interactions of sPP with 2-Quinoxalinol

The above results indicate that epitaxial crystallization of sPP on 2-Quin crystals generates the less common, chiral form II. As examined now, the preference for this less stable form rests on the structural rules that govern polymer epitaxy and actually illustrates them vividly. Furthermore, we are dealing with two structurally very similar (and simple) crystal forms of a *helical* polymer, as opposed to, e.g., the all trans chain conformation of polyethylene. The analysis takes into consideration (a) the *density* of chains in the contact plane and (b) the more subtle issue of *matching of surface topographies* of the substrate and polymer. The latter issue is of particular relevance, given the helical geometries involved.

It is known that epitaxial crystallization strongly favors *densely populated contact planes*. As indicated in the Results section, for the two *hk*0 planes with the correct 20° tilt to the crystallographic *ac* face ($(110)_{II}$ and $(120)_I$), the density of chains in $(110)_{II}$ is twice that in $(120)_I$. On this basis alone, the observed inclination of the contact plane of sPP provides a strong indication in favor of form II.

Analysis of the matching of contact planes topographies helps explain the specificity of 2-Quin for form II of sPP. The unit cell of 2-Quin is orthorhombic, with cell parameters: $a = 4.354$ Å, $b = 7.348$ Å and $c = 21.32$ Å, space group $P2_12_12_1$.[23] Earlier investigations[19,21] have shown that the contact plane is *ab*, which corresponds indeed to an easy cleavage plane. The contact face is built up by a linear array of 2-Quin molecules with their apolar benzene rings parallel to the *a* axis and tilted at some 40° to the *ab* contact plane normal. (Figure 6a). These molecules create a grating with *clearly marked parallel ditches*, 7.4 Å apart along the *b* axis. As indicated in the Introduction, the anticipated match with the ≈7.4 Å chain axis repeat distance of syndiotactic polymers was indeed the main criterion for selecting 2-Quin as a substrate in the present investigation. However, both forms I and II of sPP share this *c* axis repeat distance: on its own, this one-dimensional match provides no clue either about the exact sPP crystal form (I or II) or the specific contact plane.

A second selection criterion must therefore be operative, i.e., a dimensional/structural match in a direction transverse to the chain axis, i.e., the interchain distance in sPP. This distance must be matched along the *a* axis of 2-Quin, namely 4.354 Å, or a multiple of this value—in the present case $2a_{2\text{-Quin}} \approx 8.70$ Å. Most of the potential sPP low index *hk*0 contact planes are ruled out on the basis of poor dimensional match and/or low density of the chains in the planes: (100), interchain

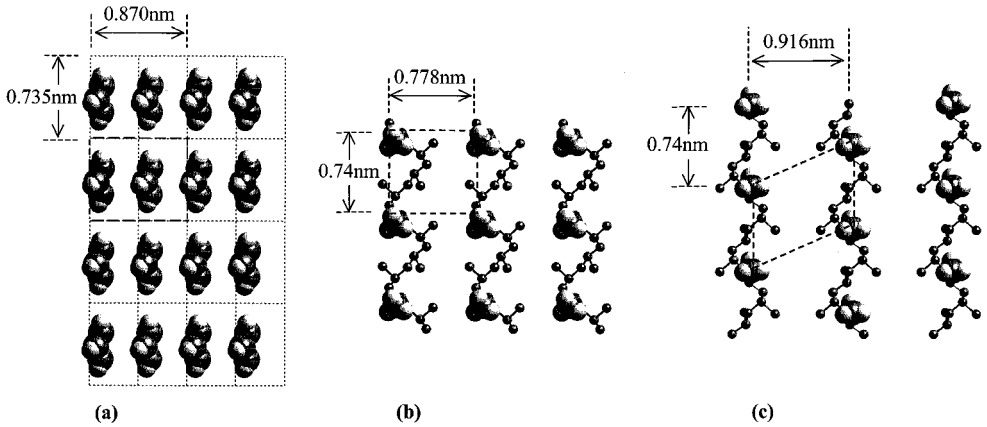

Figure 6. Structural interpretation of the prevalence of form II of sPP in the epitaxial crystallization on 2-Quin. (a) *ab* face of 2-Quin showing the rows of nearly edge-on outer parts of the benzene rings in the contact plane. Note the *b* axis periodicity of 0.735 nm, and the 0.870 nm one corresponding to two *a* repeat distances. (b) (110) contact face of sPP in its form II with the outermost methyl groups only shown in balls. Note the rectangular symmetry of the surface topography. (c) (110) contact face of sPP in form I. Although the lateral dimensional match with 2-Quin is better than for form II, the stagger of exposed methyl groups is less favorable and rules out this potential epitaxy.

distance 5.6 Å, mismatch −28%; (010), ≈14.4 Å (form II) or 7.2 Å (form I), mismatches 65.5% and −15.5%, respectively.

The two *hk*0 planes of potential interest are actually $(110)_{II}$ and $(110)_{I}$. The two planes are very similar indeed, as seen in *c* axis projection at least: they are both built up of helices of the same hand. On what type of criterion are they selected or rejected? The interchain distances are 7.77 and 9.07 Å, respectively. These distances match reasonably well with $2a_{2\text{-Quin}}$, i.e., 8.70 Å: the disregistries amount to −10.7% for form II and +4.25% for form I, respectively. The *dimensional* matching criterion would therefore favor the stable form I, but the less stable form II is produced. As examined now, *the different surface topographies* of these two potential contact faces and their matching with the substrate 2-Quin contact face provide the clue for the preference for (110) of form II.

The surface topographies of the $(110)_{II}$ and $(110)_{I}$ planes of sPP are significantly different, although the helix conformation is in both cases t_2g_2 and that in both cases *isochiral* helices are exposed (Figure 1, parts a and b, respectively). These differences arise from the different space group symmetries. The $C222_1$ symmetry of form II implies that all chains in the unit cell are located at the same height along the *c* axis. As a consequence, the topography of the layer displays a marked rectangular array with *parallel, linear ditches* 7.4 Å apart normal to the chain axis. In the $(110)_{I}$ face of sPP to the contrary, successive chains are *shifted along the c* axis: the profile of the layer displays neither the same structural regularity of ditches 7.4 Å apart nor the rectangular pattern characteristic of the $(110)_{II}$ face of sPP. These differences are vividly illustrated in Figure 6, parts b and c, in which only the outermost methyl groups (which are closest to the substrate surface) are shown in balls.

The matching *ab* contact face of 2-Quin displays a linear grating with *clearly marked linear ditches* 7.4 Å apart along the *b* axis, *and with a rectangular symmetry*. On this basis, the preference for form II and more specifically for its (110) face appears to be structurally justified by the fact that it allows for a better interaction/interdigitation of the polymer and substrate contact faces, which in a first approximation are both *rectangular* arrays 7.4 Å by ≈ 8 Å. In the present case, the dimensional matching criterion (which would favor form I) is superseded by *steric arguments* which favor definitely form II. The structural similarity of the two forms allows a clear identification of finer details of the parameters operative in the epitaxy.

5. Conclusion

Epitaxial crystallization of syndiotactic polypropylene on 2-quinoxalinol induces the less common, metastable form II, made of isochiral helices, rather than the stable antichiral form I produced in bulk crystallization. This form is produced only in a limited temperature range, at low crystallization temperatures. Furthermore, during growth away from the substrate, it converts to form I, or at least to a form I disordered to an extent characteristic of bulk crystallization at the specific T_c. This behavior reminds of a similar monoclinic to orthorhombic polyethylene growth transition[14−16] but takes place further away (>50 nm) from the substrate surface.

The structural rules that govern the epitaxy can be analyzed in some detail. The major epitaxial registry is dimensional, and involves matching of the chain axis repeat distance of sPP with the *b* parameter of 2-Quin, both ≈7.4 Å. Within this framework, several potential epitaxies with various faces of sPP in either the chiral form II or antichiral form I are possible. A second dimensional match, which involves the interchain distance, plays an important, but not an essential role. Indeed, the best match would exist for the $(110)_{I}$ face, but it is the $(110)_{II}$ contact face of the chiral form II that is selected. In ultimate analysis, the selection rests on a very favorable correspondence of the *surface topographies* of the deposit sPP $(110)_{II}$ and 2-Quin substrate contact faces: they both display regular, linear gratings of ditches 7.4 Å apart that provides for favorable interdigitation and interactions in the contact surfaces. A major structural feature of this $(110)_{II}$ sPP contact face is the fact that all the chains are *in register* along the chain axis. Other potential sPP contact planes do not display the same register and therefore structural regularity, and are never observed to become contact planes.

Acknowledgment. This work was supported by the "Special Funds for Major State Basic Research Projects",

China and by the "Association Franco-Chinoise de Coopération Scientifique et Technique" (AFCRST) under Grant "Programme de Recherches Avancées Matériaux", PRA #98.03. J.Z. is in particular thankful to the AFCRST for support of her extended stay at the ICS.

References and Notes

(1) Rodriguez-Arnold, J.; Bu, Z.; Cheng, S. Z. D. *J. Macromol. Sci.—Rev. Macromol. Chem. Phys.* **1995**, *C35*, 117.
(2) Corradini, P.; Natta, G.; Ganis, P.; Temussi, P. *J. Polym. Sci., Part C* **1967**, *16*, 2477.
(3) Lotz, B.; Lovinger, A. J.; Cais, R. E. *Macromolecules* **1988**, *21*, 2375.
(4) Lovinger, A. J.; Lotz, B.; Davis, D. D.; Padden, F. J., Jr. *Macromolecules* **1993**, *26*, 3494.
(5) Auriemma, F.; De Rosa, C.; Corradini, P. *Macromolecules* **1993**, *26*, 5719.
(6) De Rosa, C.; Auriemma, F.; Corradini, P. *Macromolecules* **1996**, *29*, 7452.
(7) De Rosa, C.; Corradini, P. *Macromolecules* **1993**, *26*, 5711.
(8) Lovinger, A. J.; Lotz, B. *J. Polym. Sci., Part B: Polym. Phys.* **1997**, *35*, 2523.
(9) Rastogi, S.; Loos, J.; Cheng, S. Z. D.; Lemstra, P. *J. Polym. Mater. Sci. Eng.* **1999**, *218*, 153.
(10) Lotz, B.; Mathieu, C.; Thierry, A.; Lovinger, A. J.; De Rosa, C.; Ruiz de Ballesteros, O.; Auriemma, F. *Macromolecules* **1998**, *31*, 9253.
(11) De Rosa, C.; Auriemma, F.; Vinti, V. *Macromolecules* **1998**, *31*, 7430.
(12) De Rosa, C.; Venditto, V.; Guerra, G.; Corradini, P. *Makromol. Chem.* **1992,** *193*, 1351.
(13) NewJapan Chemical Co, Ltd, European Patent EP 93101000.3. Japanese Patents JP 34088/92, JP 135892/92, JP 283689/92, JP 324807/92, 1992.
(14) Wittmann, J. C.; Lotz, B. *Prog. Polym. Sci.* **1990**, *15*, 909.
(15) Wellinghoff, S.; Rybnikar, F.; Baer, E. *J. Macromol. Sci. Phys.* **1974**, *B10*, 1.
(16) Wittmann, J. C.; Lotz, B. *Polymer* **1989**, *30*, 27.
(17) Rickert, E.; Baer, E. *J. Appl. Phys.* **1976**, *47*, 4304.
(18) Stocker, W.; Schumacher, M.; Graff, S.; Lang, J.; Wittmann J. C.; Lovinger, A. J.; Lotz, B. *Macromolecules* **1994**, *27*, 6948.
(19) Kopp, S.; Wittmann, J. C.; Lotz, B. *Polymer* **1994**, *35*, 908.
(20) Mathieu, C.; Stocker, W.; Thierry, A.; Wittmann, J. C.; Lotz, B; *Polymer*, in press.
(21) Mathieu, C.; Thierry, A.; Wittmann, J. C.; Lotz, B. *J. Polym. Sci., Polym. Phys. Ed.* **2000**, *38*, 3088.
(22) Cerius^2 4.2 Program, Molecular Simulations Inc., Waltham, MA, and Cambridge, UK.
(23) Padjama, N.; Ramakumar, S.; Viswamitra, M. A. *Acta Crystallogr. Sect. C* **1987**, *43*, 223921.

MA010758I